**Proceedings of the ASME 2015 International Mechanical Engineering Congress and Exposition**
**IMECE2015**
**November 13-19, 2015, Houston, Texas**

**IMECE2015-50482**



# MECHANICAL DESIGN AND INITIAL PERFORMANCE TESTING OF AN APPLE-PICKING END-EFFECTOR

**Joseph R. Davidson**
School of Mechanical and Materials Engineering
Washington State University
Richland, WA 99354, USA
joseph.davidson@wsu.edu

**Changki Mo**
School of Mechanical and Materials Engineering
Washington State University
Richland, WA 99354, USA
changki.mo@tricity.wsu.edu

## ABSTRACT

The fresh market apple industry currently relies on manual labor for all harvesting activities. The lack of mechanical harvesting technologies is a serious concern because of rising labor costs and increasingly uncertain labor availability. Researchers have been working for several decades to develop mechanical harvesters for tree fruit. The two fruit removal methods considered include mass mechanical harvesters and selective harvesting with robotics technology. Whereas mass mechanical harvesters have demonstrated unacceptable damage rates, robotic systems have been limited by insufficient speed and robustness. This paper describes the design and analysis of a novel underactuated end-effector fabricated for the robotic harvesting of tree fruit. The device has been optimized around a set of target tasks, the most critical being speed, low complexity, suitability for a highly variable field environment, and the replication of hand picking so as to minimize fruit damage. Development of the end-effector has been facilitated by a thorough study of the dynamic forces involved during the manual harvesting of apples. The end-effector produces a spherical power grasp with a normal force distribution and picking sequence replicating selected human patterns. An underactuated, tendon-driven device with compliant flexure joints has been adopted to improve system performance in the presence of position errors as well as enhance robustness to variable fruit size, shape, and orientation. The prototype end-effector also uses minimal sensors and incorporates open-loop control to reduce complexity and improve picking speed. This paper presents the theoretical analysis of the end-effector kinematics and discusses the selection of key geometric parameters. Experiments have been conducted to determine the normal forces developed during grasping of the apple. Results indicate that open-loop, feedforward control can be used to produce optimal normal force patterns.

## INTRODUCTION

In the U.S. Pacific Northwest, a large, seasonal labor-force is required for the production of tree fruit crops like fresh market apples, cherries, and pears. The most time and labor-intensive task in fruit crop production is harvesting. In Washington State alone the apple and pear harvest requires the employment of 30,000 additional workers with an estimated harvest cost of $1,100 to $2,100 USD per acre per year [1, 2]. To reduce harvesting costs and dependence on seasonal labor, researchers have developed shake-and-catch systems for the mass harvesting of fruits such as berries, cherries, and citrus [3, 4]. These techniques, which apply vibration to the trunk or branch of the tree in order to separate the fruit, are typically used to harvest fruit destined for the processing market where there are established tolerances for fruit bruising and external defects. There have been some attempts to develop mass harvesting systems for fresh market citrus, cherries, and apples, but the systems either demonstrated marginal rates of fruit detachment [5], were efficient with only compatible tree-training systems [3], or frequently harvested fruit without stems [6].

The use of robotics technology is another approach researchers have tried for the harvesting of tree fruit [7, 8]. For economic reasons related to changing labor conditions, scientists and engineers started to actively work on research and development of fruit-picking robots in the 1980s [9, 10]. These earlier research efforts defined the basic functional requirements of a fruit-picking robot as the following: i) locate the fruit on the tree in 3D dimensions; ii) approach and reach for the fruit; and iii) detach an undamaged fruit from the tree and deposit it in a container. In order for a fruit-picking robotic system to be commercially viable, it has to be economically feasible and provide harvesting rates (e.g. fruit/second) comparable to those obtained through manual harvesting. Additionally, the system should minimize damage to both the plant and the harvested fruit to a tolerable level. Despite numerous attempts to transfer industrial robotic technology directly to field based, biologically

driven environments, the mechanization of specialty crop harvesting has achieved only limited success primarily due to inadequate accuracy, speed, and robustness.

Because of rising labor costs, a high workplace injury rate due to ladder use, and increasing uncertainty about the availability of farm labor [11, 12], the lack of mechanical harvesting is a critical problem receiving much attention from both federal agencies (e.g. United States Department of Agriculture) and state and local organizations (e.g. Washington Tree Fruit Research Commission). This paper presents preliminary results from a project designed to address this problem by employing mechanization and human-machine collaboration in the production of high quality fruit for the fresh market. Previous robotic harvesting projects have identified end-effector performance, especially as it relates to robustness and limiting fruit damage, as a significant opportunity for improvement. In order to address these limitations, we propose a prototype agricultural end-effector that is based on the biological advantages and constraints that define commercial tree fruit production systems and whose design has been facilitated by a comprehensive, quantitative study of the motion and forces required during different apple picking patterns. The design and testing of the underactuated device is discussed and experimental results from grasping force measurements are presented. Performance testing of the end-effector has been completed in preparation for field tests that will integrate the robotic system's manipulator, end-effector, and machine vision system during fruit harvesting.

## NOMENCLATURE

| | |
|---|---|
| $l_1$, $l_2$ | Length of proximal and distal links |
| $k_1$, $k_2$ | Stiffness of proximal and distal flexures |
| $\boldsymbol{K}$ | Stiffness matrix |
| $r_1$, $r_2$ | Equivalent pulley radii of proximal and distal joints |
| $r_a$ | Actuator pulley radius |
| $\Delta\theta_a$ | Angular displacement of the actuator pulley |
| $\Delta\boldsymbol{\theta}$ | Configuration change of the links |
| $\boldsymbol{J}_a$ | Actuator Jacobian matrix of the finger |
| $\boldsymbol{f}_e$ | Vector of normal contact forces |
| $\boldsymbol{J}_c$ | Contact Jacobian matrix that maps between link contact forces and joint torques |
| $b_1$, $b_2$ | Location of proximal and distal normal forces |

## MANIPULATOR DESIGN

An essential step in the design of a robotic, harvesting manipulator is the creation of a kinematic framework flexible enough to accommodate the crop environment. However, the unstructured environment of agricultural fields and orchards pose unique engineering challenges compared to other automation applications. Some of these challenges include variable outdoor conditions, complex plant structures, inconsistency in product shape and size, and delicate products [13]. The most critical source of variation affecting the design of the manipulator is the highly irregular and unstructured apple tree. To improve obstacle avoidance during tree fruit harvesting a six degree of freedom (DOF) manipulator has been selected. In order to reduce costs and increase flexibility for configuration modifications, we have constructed a custom manipulator rather than purchase an off-the-shelf model. The manipulator is an open chain, serial link manipulator with revolute joints and a maximum reach of approximately 0.6 meters. It incorporates modular Dynamixel Pro actuators (Robotis Inc., Irvine, CA) and custom frames fabricated from aluminum sheetmetal. The kinematic structure of the manipulator and its associated geometric parameters are shown in Fig. 1. The recursion formulas developed by Wang and Ravani [14] are used for forward kinematics computations. Numerical solutions to the inverse kinematics problem are determined with the combined optimization method first proposed by Wang and Chen [15]. This algorithm was selected because it has been shown to be computationally efficient and does not require matrix inversion. The convergence tolerance was set at 1E-6, and the joint limits of the manipulator were used as boundary constraints. The inverse kinematics algorithm has been developed in Matlab (Mathworks Inc., Natick, MA), compiled into a C++ shared library, and integrated with the manipulator's controller in the Microsoft Visual Studio development environment. The manipulator's planned trajectory is executed using a simple, open loop look-and-move approach. In order to reduce system complexity and increase speed, visual servoing is not used.

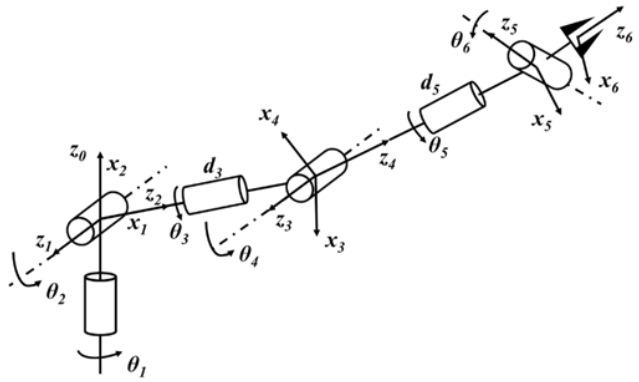


| Joint | Link Length $a$ (m) | Twist Angle $\alpha$ (degrees) | Offset Length $d$ (m) | Rotation Angle $\theta$ (degrees) |
|---|---|---|---|---|
| 1 | 0 | 90 | .177 | $\theta_1$ |
| 2 | 0 | 90 | 0 | $\theta_2$ |
| 3 | 0 | 90 | .270 | $\theta_3$ |
| 4 | 0 | 90 | 0 | $\theta_4$ |
| 5 | 0 | 90 | .219 | $\theta_5$ |
| 6 | .186 | 90 | 0 | $\theta_6$ |

Fig. 1 Kinematic configuration of the 6-DOF manipulator.

In the future systematic approaches that combine machine design and horticultural practices are required in order to improve the viability of robotic harvesting. In these systems plant characteristics, like canopy growth, tree spacing, and fruit position, are developed in conjunction with machine designs. Historically, growers were unwilling to totally transform orchards and fields to accommodate robotic harvesters because of the risks and expenses involved in making a change for an unproven technology [16]. In Washington State, the majority of new apple acreage is being planted to a two-dimensional, planer canopy supported by a wire and posts trellis system whereby most of the branches and fruit are visible and accessible to machines. This trend is in accordance with the general goal of improving productivity through the use of simple, narrow, accessible, and productive (SNAP) canopies. The authors expect that this trend of planting and training trees in an architecture with more accessible fruit will ease design requirements of the robotic harvester and help improve performance.

## END-EFFECTOR DESIGN

*Environmental Considerations*

Fruit in a single crop possess a high level of variability. For example, tree fruit vary in position, shape, size, and growing orientation. Some of this variation is shown in Fig. 2. Even for the same apple cultivar, parameters such as size and stem length vary widely within a single tree. There also exists a year-to-year variability in these parameters. This variation plays a large role in the decision to select the end-effector's fruit removal method. Because the fruit removal technique is usually the largest cause of fruit injury, it is essential that the end-effector is designed with consideration of the fruit's physical properties (e.g. friction, fruit firmness, and tensile strength of the stem). A proper understanding of these mechanical properties is important to facilitate design of the end-effector because performance is not only measured by successful removal of the fruit from the plant, but also by ensuring that the plant and fruit remain undamaged.

*Design Methodology*

The objective during design of the end-effector was to develop a prototype that replicates the human hand's manipulation methods during apple picking and addresses the constraints imposed by fruit growth habits. The end-effector has been optimized to meet a set of five specific design criteria as outlined below:

1. Detachment success of 90%. Detachment success is defined as the number of successfully harvested ripe fruit per total number of localized ripe fruit present in the manipulator's workspace.
2. Picking time of 6 seconds. This is the time required to pick and store one fruit – it does not include the time required for ripeness determination and fruit localization.
3. Damage rate to the fruit does not exceed 10%.
4. Can be used for harvesting of multiple apple cultivars.
5. Relatively lightweight, simple, and cost-effective.

The knowledge acquired during dynamic analysis of hand picking [17] has been critical during design of the end-effector. This study found that the optimal pattern to remove the fruit was to grasp the apple with the thumb and middle finger at opposite points on the equator, place the forefinger against the base of the stem, and rotate the fruit against the orientation of the stem. Compared to pulling the fruit away from the tree, this method required less force to break the stem-abscission joint and reduced the likelihood of fruit damage. Though the human grasp is a fingertip grasp, the end-effector is designed to provide a spherical, enveloping power grasp of the fruit. As some error is expected in the input provided by the machine vision system, it was determined that a power grasp would enhance robustness to position error. Likewise, dexterous manipulation of the fruit is not required. The goal is to provide a normal force distribution replicating human patterns at the proximal point of contact. The manipulator will rotate the fruit after the end-effector completes its grasp.

Fig. 2 Apples possess a high level of variation. The fruit on the left are relatively accessible and have vertical stem orientations. The fruit on the right are clustered and have inaccessible stems.

To reduce complexity a tendon-driven, underactuated design has been selected. Each end-effector finger has two links connected by flexure joints. An earlier conceptual design proposed by the authors used springs instead of flexures [18]. Underactuation and the passive compliance provided by the flexure joints provide several advantages in the unstructured orchard environment. For example, underactuation between the finger links helps to ensure a shape-adaptive grasp of fruits with variable shapes, sizes, and orientations. Also, Dollar and Howe [19] have shown with the Shape Deposition Manufacturing (SDM) hand that the passive compliance of the flexure joints increases robustness to positioning errors. In the case of unintended collisions, which are expected during harvesting, the flexure joints can sustain out-of-plane deflection and large deflections without damage [19].

The complete end-effector includes three identical fingers arranged symmetrically around a circular palm with a soft rubber insert. The spacing of the fingers was selected such that during a grasp of a sphere with diameter of 80 mm, which is a typical apple diameter, the proximal links would make contact on the fruit equator. The total length of the finger is roughly equivalent to the length of a human index finger. Each of the finger links has a soft rubber pad on the base to increase friction and therefore, tangential forces, between the end-effector and the fruit surface. Underactuation between the fingers is provided by a disc differential that is a variant of the seesaw mechanism [20]. Should a finger contact the object before the other two, the differential will rotate and enable further displacement of the remaining two tendons. There is also a gripper placed at the top of the end-effector that is intended to apply pressure against the stem during fruit detachment. At the open position the angle between the gripper links is 30 degrees. A floating pulley provides underactuation between the gripper links, each of which has a soft rubber pad. The gripper and fingers have separate actuators. The computer aided design (CAD) model of the complete end-effector is shown in Fig. 3.

*Fabrication*

The components of the end-effector were fabricated from solid models by a Replicator 2X printer (MakerBot Industries, New York). Additive manufacturing minimizes the fasteners required for assembly and lessens the total weight of the device. The fingers (Fig. 4) were printed as monolithic parts consisting of ABS plastic. Similar to the fabrication process used by Ma, Odhner, and Dollar [21], molds for the finger pads were included in the solid parts as thin shells. A soft urethane rubber (Vytaflex 30, Smooth-On, Inc.) was poured into both the finger pad cavities and the palm. After the elastomers cured the shells of the finger pad molds were cut away. Dovetail joints included on the fingers and palm holds the rubber pads in place. The flexures for the finger and gripper joints were printed with flexible filament (Ninjaflex, Fenner Drives, Inc.) and inserted directly into cavities in the links. The tendons used in the design are 100-lb, high strength fishing line. In each of the fingers the tendon is tied at the distal tip, follows a hollow channel through the links, and is routed over two small dowel pins in the proximal link in order

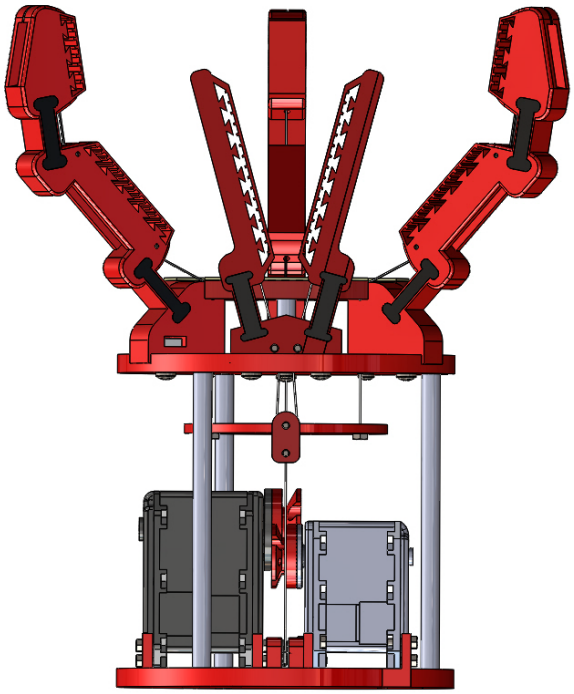

Fig. 3 Computer Aided Design (CAD) model of the prototype end-effector. The prototype is an underactuated design with three fingers and a stem gripper. Components include tendons, a disc differential, a floating pulley, a soft palm, soft finger pads (not shown), flexure joints, and two actuators.

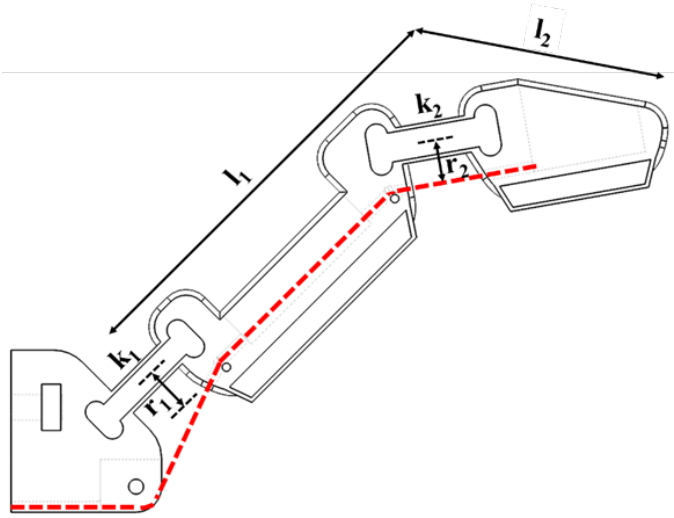


Fig. 4 Drawing of the end-effector finger. The finger has two links where $l_1$ and $l_2$ are the lengths of the proximal and distal links, respectively. The links are coupled with flexure joints having stiffness $k_i$. The routing of the tendon is shown with the dashed red line.

to reduce friction with the plastic part. There is a single, free-spinning pulley at the base of each finger that guides the tendon to its termination point on the disc differential where it is secured with a nut. The single tendon on the stem gripper is secured at

the link tips and passes over a floating pulley. The disc differential and floating pulley are attached with tendons to pulleys mounted on the horns of each actuator. The actuator pulleys, floating pulley, and differential are also printed parts. The actuators selected for the fingers and gripper are the Dynamixel MX-64AR (Robotis Inc., Irvine, CA) and MX-28AR, respectively. Dynamixel servos integrate a DC motor, reduction gearhead, PID controller, motor driver, and data network. These particular models have stall torques of 7.3 N-m (MX-64AR) and 2.5 N-m (MX-28AR). Because the operating voltage of the end-effector servos is 12VDC, it uses a separate power supply than the manipulator, which operates at 24VDC. The servos are controlled in the Microsoft Visual Studio C++ development environment using the software development kit (SDK) provided by the manufacturer.

The mass of the assembled end-effector is 0.4 kg. Based on the average mass of the apples harvested during the hand picking analysis [17], the total payload of the end-effector and harvested fruit is expected to be less than 0.7 kg. Some key geometric and physical parameters of the end-effector fingers are provided in Table 1. Note, the orthogonal distance from the midline of the flexure to the tendon entry point is used for the equivalent pulley radii. The stiffness of the flexure joints was experimentally determined. The joints were modeled as simple torsion springs, and their rotational stiffness was measured with a load cell. The stiffness ratio $k_2/k_1$ of two between the joints plays a critical role in the nature of the coupled motion between the links. The arrangement of the fingers is designed to provide a spherical power grasp fully encompassing the fruit. In this grasping sequence the proximal link makes contact with the object first before the distal link flexes to cage the fruit. Odhner et al. [22] and Dollar and Howe [19] have shown that in order to ensure this two-phased motion the distal flexure joint must be stiffer than the proximal flexure.

Table 1 Physical and geometric parameters of the end-effector prototype.

| Link | Length $l$ (m) | Joint Stiffness $k$ (N-m/rad) | Pulley Radius $r$ (m) | Resting Angle $\theta$ (°) |
|---|---|---|---|---|
| 1 | 0.07 | 0.055 | 0.00956 | 45 |
| 2 | 0.042 | 0.111 | 0.00716 | 35 |

## FORCE ANALYSIS

To reduce design complexity and enhance speed of harvesting, both of which are design criteria, the end-effector has no sensors and utilizes open-loop, feedforward control. As such, an important initial design step was to develop an environmental model for the actuation torque required to produce the desired link normal forces. Each end-effector finger is a single-acting cable-driven system with two links and two flexure joints. The flexures are modeled as simple pin joints with rotational stiffness. A more accurate model of flexure bending has been developed by Odhner and Dollar [23] and can be used to estimate beam deflection. For this prototype, which does not use sensors to detect angular positions or points of contact, we felt that modeling the flexures as pin joints with torsion springs was reasonable. Rotation of the proximal and distal links is coupled until the proximal link makes contact with the object at which point the distal link will continue to independently rotate until the system is constrained. For this cable-driven finger the kinematics of the links are coupled and may be expressed as

$$r_a \Delta\theta_a = \boldsymbol{J}_a \Delta\boldsymbol{\theta} \tag{1}$$

where $r_a$ is the radius of the actuator pulley, $\Delta\theta_a$ is the angular displacement of the actuator pulley, $\Delta\boldsymbol{\theta}$ represents the configuration change of the links, and $\boldsymbol{J}_a = (r_1 \quad r_2)$ is the actuator Jacobian of the finger. The pulley radii are represented by $r_1$ and $r_2$. The quasi-static equation of equilibrium [24, 25], which can be found with analytical mechanics and the principle of virtual work, is

$$\boldsymbol{K}\Delta\boldsymbol{\theta} + \boldsymbol{J}_c^T \boldsymbol{f}_e + \boldsymbol{J}_a^T f_a = 0 \tag{2}$$

where $\boldsymbol{K} = \begin{pmatrix} K_1 & 0 \\ 0 & K_2 \end{pmatrix}$ represents the joint stiffness of the flexures, $\boldsymbol{J}_c \in \mathbb{R}^{2\times 2}$ is the contact Jacobian that maps between contact forces acting on the finger and the joint torques, $\boldsymbol{f}_e = \begin{pmatrix} f_1 \\ f_2 \end{pmatrix}$ represents the normal contact force on the proximal and distal links, and $f_a$ is the actuator force. For this two-link mechanism the contact Jacobian $\boldsymbol{J}_c$ is [26]

$$\boldsymbol{J}_c = \begin{pmatrix} b_1 & 0 \\ b_2 + l_1 \cos\theta_2 & b_2 \end{pmatrix} \tag{3}$$

where $b_1$ is the proximal force location, $b_2$ is the distal force location, and $l_1$ is the proximal link length. The normal forces can then be found by

$$\boldsymbol{f}_e = \boldsymbol{J}_c^{-T}(-\boldsymbol{K}\Delta\boldsymbol{\theta} - \boldsymbol{J}_a^T f_a) \tag{4}$$

In most grasps the proximal normal force will be located on or about the fruit's equator. The problem required is to determine the actuation force that produces the normal forces of human picking patterns. In reality, this is a complicated process because the normal forces are highly dependent upon the final kinematic configuration of the underactuated finger. During harvesting operations position errors and variation in fruit shape and size will lead to numerous end-effector grasp configurations. Likewise, in some configurations negative normal forces may develop, which indicates loss of contact of the respective link [26]. The actuation force input provided with open-loop control should ensure that in all possible configurations the final grasp does not damage the fruit. A Matlab simulation (Mathworks Inc., Natick, MA) was conducted to examine the effect of position error on the proximal normal force. The center of a circle with

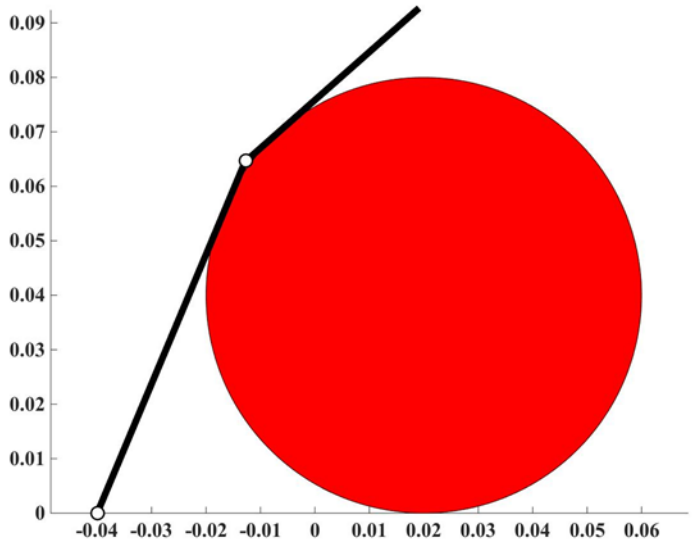


Fig. 5 Example grasp configuration from a Matlab solver used to determine angles of link rotation and points of normal contact for various fruit positions.

diameter of 80 mm was placed at different positions in the x-y plane having an error ranging from – 10 to + 10 mm in the x-direction and 0 to 10 mm in the y-direction. The grid included a total of 400 different fruit position points. At each point it was assumed that the fruit was constrained by the stem/branch system. The simulation used a solver to estimate the configuration where the finger links were tangent to the circle and then determined the change in link positions $\Delta\boldsymbol{\theta}$ and the points of contact $b_1$ and $b_2$ assuming a single point of contact on each link. An example of an equilibrium grasp configuration calculated by the solver is shown in Fig. 5. The resulting proximal normal force was then determined with eqn. (4). Tangential forces due to friction were not considered. The presence of tangential forces should theoretically increase the pullout force required to remove the fruit from the end-effector's grasp. The results of the simulation are shown in Fig. 6. The force data, which is scaled with unity-based normalization, shows that for a constant actuation force the proximal normal force is greater for increasing $\Delta\theta_1$. As shown in Fig. 5, the x-positon of the finger base is located at -.04 m. For increasing values of x the fruit moves away from the finger base and the proximal link must rotate further in order to contact the fruit. Aukes et al. [27] have created vector fields for the total resultant force on an object by superimposing force data from two planar fingers in an opposed grasp. By superimposing the data from each of the three fingers the greatest resultant force can be expected near the center of the end-effector at a small distance away from the palm. Results from experimental testing designed to explore the relationship between actuation force and normal contact forces are discussed in the following section.

## EXPERIMENTAL TESTING

Normal forces were experimentally measured during a grasp of a plastic sphere with radius of 40 mm. The sphere was located symmetrically with respect to the end-effector, meaning the centerline of the end-effector was coincident with the center of the sphere resting on the palm. Three piezoresistive force sensors (Tekscan Inc., Boston, MA) were attached to the contact locations on the proximal links. To complete a power grasp the end-effector's actuator, which is nonbackdriveable, was operated in torque mode and driven to its stall point. The normal force was then measured at static equilibrium. This measurement was repeated for increasing actuator loads. A picture of the experimental set-up is provided in Fig. 7. The same experiment

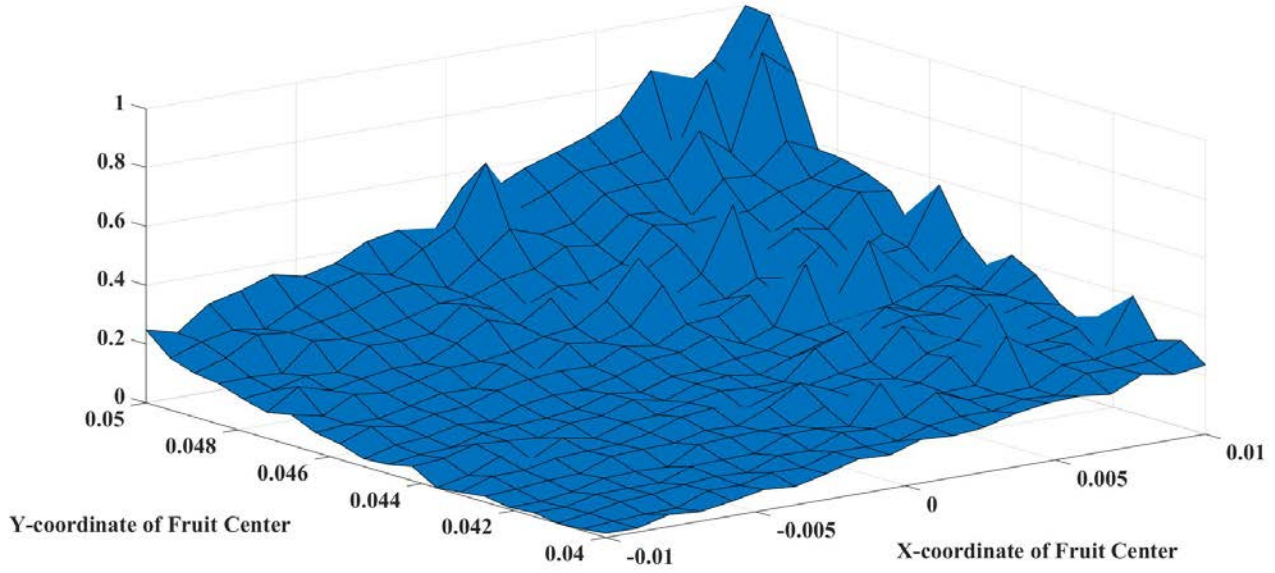


Fig. 6 The normalized proximal force that develops at static-equilibrium for a single finger. The x-y coordinate represents the position of the center of a circle with radius of 40 mm.

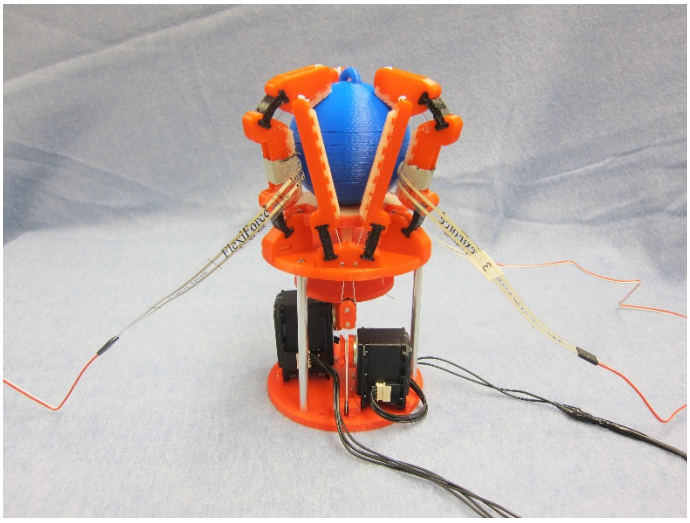

Fig. 7 Experimental set-up for contact force measurement. The actuator was driven to its stall torque and the contact force was then measured with force sensitive resistors (FSR).

was also repeated for the distal normal forces. The experimental results for the normal force measurements at five different actuator loads are shown in Fig. 8. As expected, for increasing tendon tension the proximal normal force is significantly higher than the distal force. While the change in proximal force is relatively linear for increasing tendon tension, the change in distal force is highly irregular and shows sharp jumps interspersed with horizontal slopes. The proximal links remain static once contact with the surface is made, however, the distal links often adjusted their equilibrium configurations at new actuator loads. Figure 9 shows a comparison of the proximal normal forces measured for the three fingers simultaneously at ten different actuator loads. The results present the mean values from six different iterations. For this particular grasp approximately 10% of the actuator's maximum torque value was required to produce proximal normal forces representative of those developed during manual picking of apples, which is approximately 7 N. Based on the simulation results presented in Fig. 6, the contact forces developed with this actuation torque for asymmetric grasp configurations should remain below the 11 N force threshold that caused bruising during field tests of hand-picking patterns. Whether this control input developed through experimental analysis of a symmetric grasp can successfully remove fruit from the tree, considering the external disturbance provided by the stem's tensile and rotational strength, in asymmetric configurations will be a subject of future study. Though the normal force distribution was similar for each of the fingers, the grasp was not force-isotropic as would be expected for a symmetric grasp. Because normal forces are highly configuration dependent, slight variations in the sensor placement can significantly impact the final results. Also, when increasing tendon tension the point of proximal contact

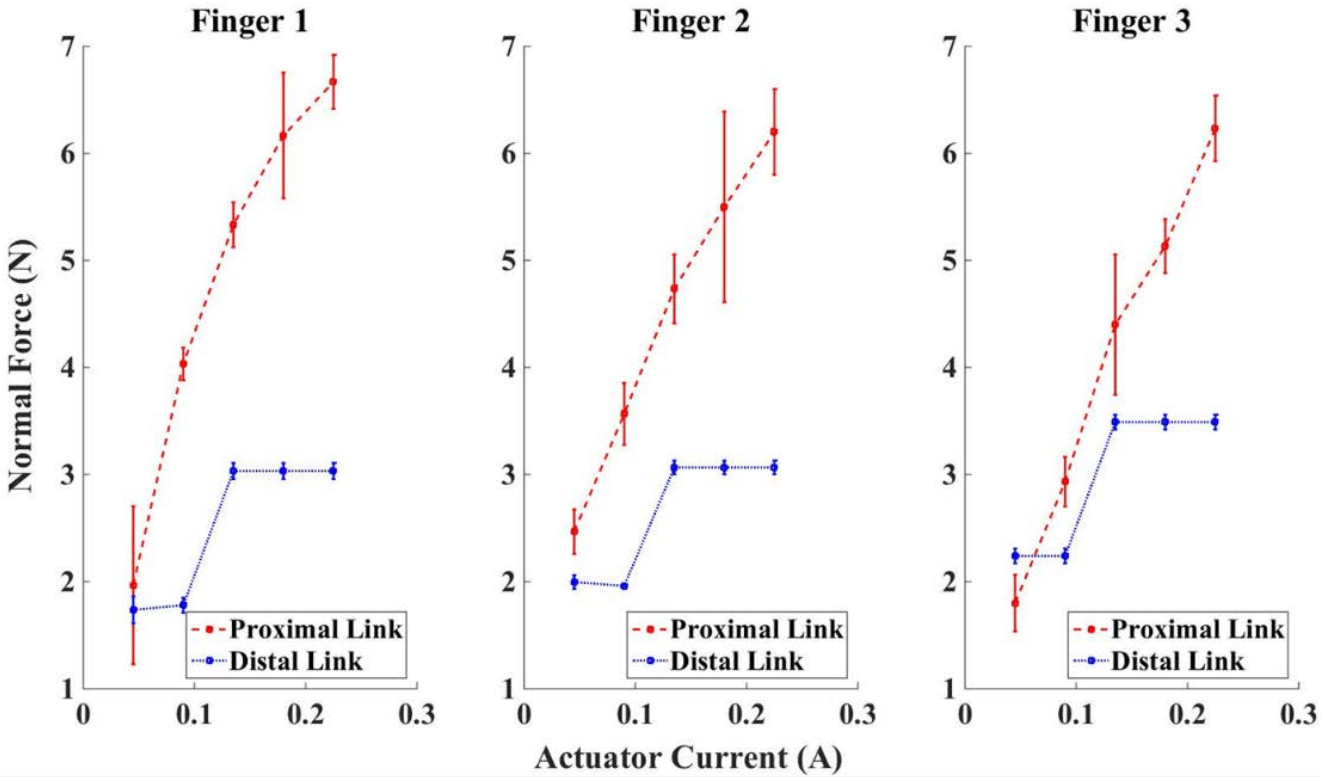


Fig. 8 Proximal and distal normal forces are compared at five different actuator loads for each finger. The data points represent the mean values of three different iterations and the error bars present standard deviation.

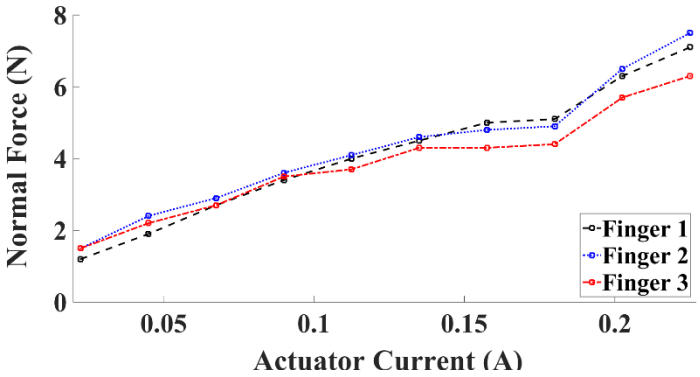


Fig. 9 The proximal link normal forces that develop during a power grasp of a sphere with a diameter of 80 mm. The normal forces are plotted versus the actuator load.

sometimes slightly adjusted. The change in position of normal contact relative to the sensor may be a source of some of the variance between the proximal force values. Finally, at higher actuation loads there was a tendency for some of the outer layers on the proximal flexures to delaminate. This process could cause inconsistencies between joint stiffness and may also be another source of force variances. The authors intend to address delamination of the flexures by adjusting part orientation and other printing parameters during the manufacturing process.

## CONCLUSION

This paper presented the design of a prototype end-effector built for the robotic harvesting of tree fruit. An underactuated design using flexure joints with passive compliance has been adopted in order to increase robustness to position error, which has been a significant limitation of previous fruit harvesting end-effectors. The device uses open-loop control, provides a shape-adaptive grasp, and produces contact forces similar to those used during optimal hand picking patterns. Other benefits of the design include its relatively low weight, low cost, and simple design. A picture of the end-effector/manipulator system completing a grasp of a replica apple is shown in Fig. 10. Future work will include analysis of the end-effector's robustness to position error. Experiments will be conducted to quantify the acceptable error during fruit localization, which will be completed by a separate vision system. The ability of the end-effector to maintain a secure grasp in the presence of external torque disturbances representing the rotational strength of the stem is another subject of future study. Preliminary results indicate that the end-effector can maintain its grasp of the fruit when subjected to pulling forces in excess of 35 N directed along the normal axis of the device. Field tests in a production apple orchard are scheduled. These integrated tests will use quantitative performance measures to determine the ability of the machine vision system, manipulator, and proposed end-effector to successfully harvest fresh market apples.

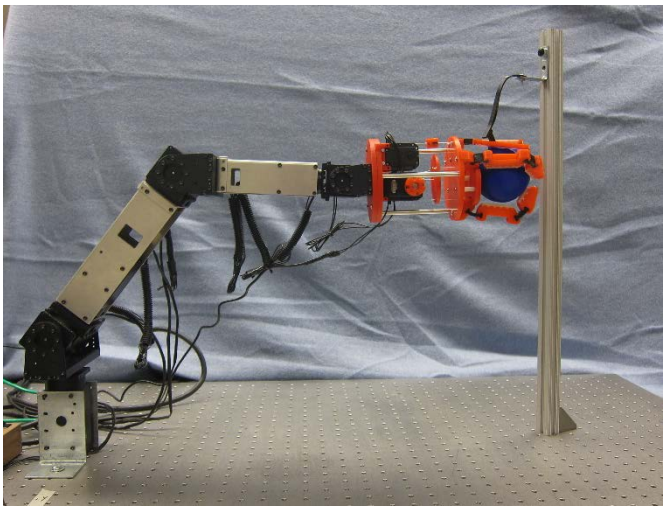

Fig. 10 End-effector mounted on the manipulator. The robot is completing a grasp of a replica apple, stem, branch system.

## ACKNOWLEDGMENT

This work was supported by the United States Department of Agriculture-National Institute of Food and Agriculture (USDA-NIFA) through the National Robotics Initiative (NRI).

## REFERENCES

[1] R. K. Gallardo, M. Taylor and H. Hinman, "2009 Cost Esimates of Establishing and Producing Gala Apples in Washington (FS005E)," 2010.

[2] S. Galinato and R. K. Gallardo, "2010 Estimated Cost of Producing Pears in North Central Washington (FS031E)," 2011.

[3] D. L. Peterson, M. D. Whiting and S. D. Wolford, "Fresh-Market Quality Tree Fruit Harvester Part I: Sweet Cherry," Applied Engineering in Agriculture, vol. 19, no. 5, pp. 539-543, 2003.

[4] R. Polat, I. Gezer, M. Guner, E. Dursun, D. Erdogan and H. Bilim, "Mechanical Harvesting of Pistachio Nuts," Journal of Food Engineering, vol. 79, pp. 1131-1135, 2007.

[5] A. Torregrosa, E. Orti, B. Martin, J. Gil and C. Ortiz, "Mechanical Harvesting of Oranges and Mandarins in Spain," Biosystems Engineering, vol. 104, pp. 18-24, 2009.

[6] D. L. Peterson and S. D. Wolford, "Fresh-Market Quality Tree Fruit Harvester Part II: Apples," Applied Engineering in Agriculture, vol. 19, no. 5, pp. 545-548, 2003.

[7] J. Baeten, K. Donne, S. Boedrij, W. Beckers and E. Claesen, "Autonomous Fruit Picking Machine: A Robotic Apple Harvester," Field and Service Robotics, vol. 42, pp. 531-539, 2008.

[8] D. Zhao, J. Lu, W. Ji, Y. Zhang and Y. Chen, "Design and Control of an Apple Harvesting Robot," Biosystems Engineering, vol. 110, pp. 112-122, 2011.

[9] A. Grand D'Esnon, "Robotic Harvesting of Apples," in Proceedings of Agri-Mation 1. ASAE Paper 1-85, St. Joseph, MI, 1985.

[10] R. C. Harrell and P. Levi, "Vision Controlled Robots for Automatic Harvesting of Citrus," in International Conference on Agricultural Engineering, Paper No. 88.426, Paris, France, 1988.

[11] S. A. Fennimore and D. J. Doohan, "The Challenges of Specialty Crop Weed Control," Weed Technology, pp. 364-372, 2008.

[12] L. Calvin and P. Martin, "The U.S. Produce Industry and Labor: Facing the Future in a Global Economy," Economic Research Service, United States Department of Agriculture (USDA), 2010.

[13] M. Karkee and Q. Zhang, "Mechanization and Automation Technologies in Specialty Crop Production," ASABE Resource Magazine, pp. 16-17, September/October 2012.

[14] L. T. Wang and B. Ravani, "Recursive Computations of Kinematic and Dynamic Equations for Mechanical Manipulators," IEEE Journal of Robotics and Automation, Vols. RA-1, no. 3, pp. 124-131, 1985.

[15] L. T. Wang and C. C. Chen, "A Combined Optimization Method for Solving the Inverse Kinematics Problem of Mechanical Manipulators," IEEE Transactions on Robotics and Automation, vol. 7, no. 4, pp. 489-499, August 1991.

[16] G. Muscato, M. Prestifilippo, N. Abbate and I. Rizzuto, "A Prototype of an Orange Picking Robot: Past History, the New Robot and Experimental Results," Industrial Robot: An International Journal, vol. 32, no. 2, pp. 128-138, 2005.

[17] J. Tong, Q. Zhang, M. Karkee, H. Jiang and J. Zhou, "Understanding the Dynamics of Hand Picking Patterns of Fresh Market Apples," in ASABE and CSBE/SCGAB Annual International Meeting, Montreal, Canada, 2014.

[18] J. R. Davidson and C. Mo, "Conceptual Design of an End-Effector for an Apple Harvesting Robot," in Conference on Automation Technology for Off-Road Equipment (ATOE), Beijing, China, September 16-19, 2014.

[19] A. M. Dollar and R. D. Howe, "The Highly Adaptive SDM Hand: Design and Performance Evaluation," The International Journal of Robotics Research, vol. 29, no. 5, pp. 585-597, April 2010.

[20] S. Hirose, "Connected Differential Mechanism and its Applications," in Proceedings of the 1985 International Conference on Advanced Robotics, Tokyo, Japan, September 1985.

[21] R. R. Ma, L. U. Odhner and A. M. Dollar, "A Modular, Open-Source 3D Printed Underactuated Hand," in IEEE International Conference on Robotics and Automation, Karlsruhe, Germany, 2013.

[22] L. U. Odhner, L. P. Jentoft, M. R. Claffee, N. Corson, Y. Tenzer, R. R. Ma, M. Buehler, R. Kohout, R. D. Howe and A. M. Dollar, "A Compliant, Underactuated Hand for Robust Manipulation," The International Journal of Robotics Research, vol. 33, no. 5, pp. 736-752, 2014.

[23] L. U. Odhner and A. M. Dollar, "The Smooth Curvature Model: An Efficient Representation of Euler-Bernoulli Flexures as Robot Joints," IEEE Transactions on Robotics, vol. 28, no. 4, pp. 761-772, 2012.

[24] D. M. Aukes, "PHD Dissertation: Design and Analysis of Selectively Compliant Underactuated Robotic Hands," Stanford University, 2013.

[25] R. Balasubramanian and A. M. Dollar, "Variation in Compliance in Two Classes of Two-Link Underactuated Mechanisms," in IEEE International Conference on Robotics and Automation, Shanghai, China, 2011.

[26] L. Birglen and C. M. Gosselin, "Kinetostatic Analysis of Underactuated Fingers," IEEE Transactions on Robotics and Automation, vol. 20, no. 2, pp. 211-221, 2004.

[27] D. Aukes, S. Kim, P. Garcia, A. Edsinger and M. R. Cutkosky, "Selectively Compliant Underactuated Hand for Mobile Manipulation," in IEEE International Conference on Robotics and Automation, Saint Paul, Minnesota, USA, 2012.